

# Potential curves for the ground and numerous highly excited electronic states of $K_2$ and NaK

S. Magnier<sup>1,\*</sup> and Ph. Millié<sup>2</sup>

<sup>1</sup>Laboratoire Aimé Cotton, CNRS II, Bâtiment 505, Campus d'Orsay, 91405 Orsay Cedex  
and <sup>2</sup>DRECAM/SPAM, Centre d'Étude de Saclay, 91191 Gif-sur-Yvette, France

(Received 16 March 1995; revised manuscript received 18 September 1995)

Potential curves of the  $K_2$  and NaK molecules have been computed in the framework of pseudopotential methods, over a wide range of internuclear distances. At short internuclear distances, the agreement with experimental data is excellent, the mean deviation between theoretical and experimental spectroscopic constants being 1% for the two alkali dimers. At large internuclear separation, wells and avoided crossings are observed in adiabatic potential curves of highly excited states correlated to the asymptotes close to  $K[4p] + K[4p]$  and  $Na[3p] + K[4p]$ . For example, the well depths of the  $^1\Sigma^+$  states reach  $2650\text{ cm}^{-1}$  for  $K_2$  and  $4330\text{ cm}^{-1}$  in the case of NaK. We demonstrate that they correspond to pseudocrossings between covalent states (dissociating into  $K[nl] + K[n'l']$  or  $Na[nl] + K[n'l']$ ) and ionic states (correlated to  $K^+ + K^-$  for  $K_2$ ,  $Na^+ + K^-$ , or  $Na^- + K^+$  for NaK, the negative ion being in the ground state or an autoionizing state). As for  $Na_2$ , these structures may play a crucial role in the interpretation of low-energy collisions. [S1050-2947(96)05905-8]

PACS number(s): 31.15.Ar; 31.50.+w; 33.20.-t

## I. INTRODUCTION

During the past decade, an important experimental effort has been devoted to the laser spectroscopy of the ground and excited states of the  $Na_2$ ,  $K_2$ , and NaK alkali dimers: spectroscopic constants and potential curves of 27 electronic states of the  $Na_2$  molecule have been determined (see [1] and references therein), while 17 electronic states of  $K_2$  [2–14] and nine of NaK [15–27] are presently known with a high accuracy. Recently, highly excited states of  $Na_2$  and  $K_2$ , dissociating close to the  $Na[3p] + Na[3p]$  and  $K[4p] + K[4p]$  doubly excited asymptotes, were observed by Stwalley and co-workers, with optical-optical double-resonance techniques (Refs. [4, 28, 29]). Moreover, with the development of laser cooling and optical trapping techniques (Ref. [30] and references therein), the knowledge of molecular potential curves at short and mainly at large internuclear distances has become crucial in the interpretation of low-energy atom-atom collisions.

These experimental activities have stimulated theoretical developments to compute relevant adiabatic potential curves, especially in the framework of model potential (Refs. [31] and [32]) or pseudopotential (Refs. [33–38]) methods. For all these methods, alkali dimers are treated as systems with two active electrons moving in a field of two ionic cores, where core valence electron interactions are represented by an effective potential. In the model potential method, the formalism of Bottcher and Dalgarno [39] has been used while in the pseudopotential methods three approaches [38,40,42] have been proposed for the calculations of core-polarization effects and of the correlation energy between the core and valence electrons. The first [40] is perturbative, and generally leads to an overestimation of the dissociation en-

ergies and an underestimation of equilibrium distances which are shorter than the experimental values by  $0.6a_0$  when a large basis set is used [41]. The second approach [42] is totally different; it simply adds a semiempirical core-polarization potential to the valence electrons Hamiltonian. A cutoff function is then introduced to deal with the interaction effects at short range, and to overcome computational difficulties. The third approach [38] is derived from the preceding one using the same core-polarization potential though now with an  $l$ -dependent cutoff function. Calculations through this approach have recently been compared to results from a model potential method in the case of the sodium dimer for which the ground and many excited states (Refs. [1] and [43]) have been determined. A very good agreement between these two methods and with experiment has been demonstrated, the mean deviation between theoretical and available experimental spectroscopic constants being  $\Delta R_e = 0.05a_0$ ,  $\Delta w_e = 0.86\text{ cm}^{-1}$ ,  $\Delta T_e = 76\text{ cm}^{-1}$ , and  $\Delta D_e = 57\text{ cm}^{-1}$ . One of the most interesting results in our investigation of  $Na_2$  is the occurrence of structures at large internuclear separation for the  $^1\Sigma^+$  and  $^3\Pi$  symmetries. For example, we predicted a well located at  $R = 26a_0$ , with a depth of  $952\text{ cm}^{-1}$  for the  $5^1\Sigma_g^+$  excited state correlated to  $Na[3s] + Na[4p]$  [43], while Tsai, Bahns, and Stwalley [29] recently observed this minimum at  $R = 26.19a_0$ , and found a depth of  $983\text{ cm}^{-1}$ . Thus their results have confirmed our predictions and the accuracy of our calculations at large internuclear separations.

Following our investigations of alkali dimers, we investigated many states of  $K_2$  and NaK over a wide range of internuclear distances, using the same pseudopotential method [38] as previously used to describe  $Cs_2$ ,  $Rb_2$ , and  $Na_2$ . In contrast to  $Na_2$ , few calculations have been performed on these two molecules: Müller and Meyer [37] presented the spectroscopic constants of the ground state for these molecules and their cations, while Krauss and Stevens [44] computed the potential curves of the two states dissociating into

\*Present address: Laboratoire de Spectrométrie Ionique et Moléculaire, CNRS URA No. 171, Bât. 205, Université Claude Bernard Lyon I, 69622 Villeurbanne Cedex, France.

TABLE I. Molecular GTO basis set used for the potassium atom.

<i>s</i> orbitals		<i>p</i> orbitals		<i>d</i> orbitals		<i>f</i> orbitals	
exponent	coefficient	exponent	coefficient	exponent	coefficient	exponent	coefficient
0.931 20	0.024 63	0.133 00	1	1.255 00	0.027 54	0.015	1
0.267 60	-0.262 80	0.051 28	1	0.443 20	0.053 91	0.005	1
0.041 70	1	0.016 42	1	0.109 00	0.108 30		
0.028 15	1	0.005 20	1	0.029 94	1		
0.014 48	1	0.002 20	1	0.010 13	1		
0.005 50	1			0.003 70	1		
0.002 60	1			0.001 80	1		

$K[4s]+K[4s]$ . Jeung and co-workers [35,36] extended their calculations to the lowest excited states correlating to asymptotes up to  $K[4s]+K[3d]$  and  $Na[3p]+K[4s]$ , and Stevens, Konowalow, and Ratcliff [45] determined those of the electronic states dissociating up to the  $Na[3s]+K[3d]$  asymptote. Recently, Ilyabaev and Kaldor [46] developed an open-shell coupled-cluster method, and described the two first dissociation limits of  $K_2$ ,  $K[4s]+K[4s]$ , and  $K[4s]+K[4p]$ . Nevertheless, to our knowledge no investigations have been performed for highly excited states, and their descriptions constitute a challenge for theoreticians.

The main purpose of this work is to report information on the highly excited states of these molecules in order to interpret collisional processes between two excited atoms, such as the energy pooling reaction studied by Allegrini and co-workers [47,48] or the associative ionization reaction only observed experimentally for  $K_2$  [48–50]. Atomic units will be used except when otherwise stated.

## II. METHOD

Basically we use the same pseudopotential method as in our previous work on  $Na_2$  or  $Cs_2$  and  $Rb_2$  [1,38]. The Na and K atoms are treated through the one-electron pseudopotential proposed by Barthelat and Durand [51]. In this approach, the electron-core interaction is represented by the effective potential

$$V[r]=\sum_{l=0}^2 U_l[r]P_l. \quad (1)$$

In (1),  $l$  is the orbital angular momentum, and  $P_l$  corresponds to the projection operator on the subspace defined by the  $Y_m^l$  spherical harmonics with a given  $l$ . The pseudopotentials  $U_l[r]$  are written as

$$U_l[r]=\sum_{i=1}^2 c_i r^{n_i} \exp[-\alpha_i r^2], \quad (2)$$

where  $c$ ,  $n$ , and  $\alpha$  are adjusted to fit the energy and wave functions of the valence Hartree-Fock orbitals. Details of the sodium and potassium atoms are presented in the paper by Maynau and Daudey [52].

For Na, we used the same basis set of Gaussian-type orbitals (GTO's) as in our work on  $Na_2$  [1]. For K, the Gaussian basis set used is built up from that defined by Jeung and Ross [35], by adding more diffuse orbitals necessary for the

description of highly excited states. Presently the basis set of the potassium atom consists of six  $s$ , five  $p$ , five  $d$ , and two  $f$  Gaussian functions which are sufficient to reproduce correctly the ten first atomic levels up to  $K[5d]$ . Data are reported in Table I for the potassium atom, while those for sodium are given in Ref. [1].

The core-polarization effects are described by the effective potential proposed by Müller, Flesch, and Meyer [42]:

$$V_{cpp}=\frac{-1}{2}\sum_{\lambda}\alpha_{\lambda}\mathbf{f}_{\lambda}\cdot\mathbf{f}_{\lambda}, \quad (3)$$

where  $\alpha_{\lambda}$  is the dipole polarizability of the ionic core  $\lambda$ . They have been taken to be equal to the experimental ones (respectively  $0.9947a_0$  for  $Na^+$  and  $5.354a_0$  for  $K^+$  [37]). The electric field  $\mathbf{f}_{\lambda}$ , which acts on the atom  $\lambda$ , is due to the valence electrons and the other core, and is modified by the  $l$ -dependent cutoff function  $F$  defined in Ref. [38],

$$\sum_{l=0}^{\infty}\sum_{m=-l}^{+l}F_l(r_{i\lambda},\rho_{\lambda}^l)|lm\lambda\rangle\langle lm\lambda|. \quad (4)$$

In (4),  $|lm\lambda\rangle$  corresponds to the spherical harmonic centered on the atom  $\lambda$ , and the cutoff function  $F_l$  is written as

$$F_l(r_{i\lambda},\rho_{\lambda}^l)=\begin{cases} 0, & r_{i\lambda}<\rho_{\lambda}^l \\ 1, & r_{i\lambda}>\rho_{\lambda}^l \end{cases}. \quad (5)$$

For atoms with a single valence electron, each cutoff parameter  $\rho_{\lambda}^l$  can be independently fitted to the ionization potential and transition energies. The cutoff radii  $\rho_{\lambda}^l$  are adjusted to fit

TABLE II. Spectroscopic constants for the ground state of the  $K_2^+$  and  $NaK^+$  molecular ions.

	(Units of $R_e/a_0$ )	$\omega_e$ (cm <sup>-1</sup> )	$D_e$ (cm <sup>-1</sup> )
$X^2\Sigma_g^+(K_2^+)$			
Experiment (Ref. [54])	8.68	73.40	6670
Theory (Ref. [37])	8.60	72.40	6573
Theory (Ref. [46])	8.53	73.70	6589
Present work	8.47	73.70	6690
$X^2\Sigma^+(NaK^+)$			
Experiment (Ref. [55])			4645
Theory (Ref. [37])	7.71	91.90	4581
Present work	7.65	91.00	4645

TABLE III. Spectroscopic constants and adiabatic dissociation limits for 61 electronic states of  $K_2$ , including comparison with available experimental data.

State	Determination	$R_e$ (units of $a_0$ )	$T_e$ ( $\text{cm}^{-1}$ )	$\omega_e$ ( $\text{cm}^{-1}$ )	$D_e$ ( $\text{cm}^{-1}$ )	Dissociation limit $K[nl]+K[n'l']$
$1^1\Sigma_g^+$						$4s+4s$
	Expt. (Ref. [2])	7.42	0	92.40	4451	
	Expt. (Ref. [3])	7.42	0	92.40	4440	
	Theory (Ref. [44])	7.44	0	88.40	4267	
	Theory (Ref. [37])	7.45	0	91.80	4331	
	Theory (Ref. [35])	7.62	0	87.17		
	Theory (Ref. [46])	7.29	0	96.68	4283	
Present work	7.39	0	93.18	4289		
$2^1\Sigma_g^+$						$4s+4p$
	Theory (Ref. [35])	9.92	14 685	45.10		
	Present work	9.63	14 343	45.76	2969	
$3^1\Sigma_g^+$						$4s+5s$
	Theory (Ref. [35])	9.87	20 524	32.82		
	Present work	8.61	20 319	29.55	4988	
$4^1\Sigma_g^+$						$4s+3d$
	Theory (Ref. [35])	9.47	21 279	75.09		
	Present work	8.98	21 378	84.95	4447	
$5^1\Sigma_g^+$						$4s+5p$
	Expt. (Ref. [4])	8.46	25 376	69.77	3793	
	Present work	8.57	25 276	71.18	3764	
$6^1\Sigma_g^+$						$4p+4p$
	Expt. (Ref. [4])	8.40	25 882	72.75	4621	
	Present work	8.39	25 790	73.52	4545	
$7^1\Sigma_g^+$ inner						$4p+4p$
	Present work	8.57	27 942	26.47	2392	
$7^1\Sigma_g^+$ outer	Present work	10.79	27 931	68.42	2403	
$8^1\Sigma_g^+$						$4s+4d$
	Present work	8.56	28 042	71.22	3664	
$9^1\Sigma_g^+$						$4s+6s$
	Expt. (Ref. [4])	8.45	28 233	70.03	3673	
	Present work	8.47	28 184	69.32	3557	
$1^1\Sigma_u^+$						$4s+4p$
	Expt. (Ref. [5])	8.60	11 108	70.55	6328	
	Theory (Ref. [50])	8.64	10 634	72.28	6130	
	Theory (Ref. [39])	8.94	11 168	67.57		
	Present work	8.57	11 010	70.42	6302	
$2^1\Sigma_u^+$ inner						$4s+5s$
	Theory (Ref. [39])	8.86	22 028	24.30		
	Present work	9.27	21 922	40.45	3385	
$2^1\Sigma_u^+$ outer						
	Expt. (Ref. [6])		21 701	25.98	3772	
	Present work	14.05	21 594	29.67	3713	
$3^1\Sigma_u^+$						$4s+3d$
	Expt. (Ref. [7])	8.91	23 863	63.41	2123	
	Theory (Ref. [39])	9.49	23 283	55.06		
	Present work	8.84	23 541	62.09	2284	
$4^1\Sigma_u^+$						$4s+5p$
	Present work	8.74	26 469	21.05	2571	
$5^1\Sigma_u^+$						$4s+4d$
	Present work	8.56	27 259	69.31	4448	

TABLE III. (Continued).

State	Determination	$R_e$ (units of $a_0$ )	$T_e$ ( $\text{cm}^{-1}$ )	$\omega_e$ ( $\text{cm}^{-1}$ )	$D_e$ ( $\text{cm}^{-1}$ )	Dissociation limit $\text{K}[nl] + \text{K}[n'l']$
$6^1\Sigma_u^+$	Present work	9.92	28 334	66.73	3407	$4p + 6s$
$1^3\Sigma_g^+$	Theory (Ref. [39])	9.58	13 365	56.60		$4s + 4p$
	Present work	8.99	13 534	59.85	3778	
$2^3\Sigma_g^+$	Theory (Ref. [39])	8.49	19 732	74.04		$4s + 5s$
	Present work	8.07	19 350	80.91	5957	
$3^3\Sigma_g^+$	Theory (Ref. [39])	8.93	23 267	68.34		$4s + 3d$
	Present work	8.49	23 535	71.46	2289	
$4^3\Sigma_g^+$	Present work	8.33	25 666	75.37	3491	$4s + 5p$
$5^3\Sigma_g^+$	Present work	8.51	27 081	68.28	4625	$4s + 4d$
$6^3\Sigma_g^+$	Present work	8.60	28 036	66.40	3705	$4s + 6s$
$1^3\Sigma_u^+$	Expt. (Ref. [8])	10.91	4196	21.76	254	$4s + 4s$
	Theory (Ref. [46])	10.00	4192	28.65	89	
	Theory (Ref. [44])	11.01	4193	20.50	258	
	Theory (Ref. [35])	10.83	4043	23.14		
	Present work	10.84	4057	20.81	232	
	dissociative state					
$2^3\Sigma_u^+$						$4s + 4p$
$3^3\Sigma_u^+$	Theory (Ref. [35])	10.78	21 727	55.79		$4s + 5s$
	Present work	9.98	21 742	72.15	3566	
$4^3\Sigma_u^+$	Theory (Ref. [35])	9.78	23 716	70.35		$4s + 3d$
	Present work	9.32	24 158	65.65	1666	
$5^3\Sigma_u^+$	Present work	8.53	26 297	70.53	2743	$4s + 5p$
$6^3\Sigma_u^+$	Present work	8.60	27 349	68.72	2986	$4p + 4p$
$7^3\Sigma_u^+$	Present work	8.48	28 631	72.31	1704	$4p + 4p$
$8^3\Sigma_u^+$	Present work	8.62	29 323	65.93	2383	$4s + 4d$
$1^1\Pi_u$	Expt. (Ref. [9])	8.00	15 377	74.89	2094	$4s + 4p$
	Theory (Ref. [46])	8.13	15 711	73.54	1057	
	Theory (Ref. [35])	8.40	15 684	67.85		
	Present work	8.01	15 421	74.05	1891	
$2^1\Pi_u$	Expt. (Ref. [10])	8.35	22 970	61.50	3016	$4s + 3d$
	Theory (Ref. [35])	9.00	23 062	48.37		
	Present work	8.42	23 105	60.11	2719	
$3^1\Pi_u$	Expt. (Ref. [7])	8.84	23 927	62.70	5238	$4s + 5p$
	Present work	8.64	23 855	74.19	5186	
$4^1\Pi_u$	Expt. (Ref. [11])	8.57	26 487	62.08	3991	$4p + 4p$
	Present work	8.58	26 417	63.99	3918	

TABLE III. (Continued).

State	Determination	$R_e$ (units of $a_0$ )	$T_e$ ( $\text{cm}^{-1}$ )	$\omega_e$ ( $\text{cm}^{-1}$ )	$D_e$ ( $\text{cm}^{-1}$ )	Dissociation limit $K[nl]+K[n'l']$
$5^1\Pi_u$	Present work	8.59	27 351	73.13	4355	$4s+4d$
$1^1\Pi_g$	Expt. (Ref. [12])	9.74	16 204	34.04	1261	$4s+4p$
	Theory (Ref. [35])	9.87	15 905	40.69		
	Present work	9.73	16 063	33.45	1248	
$2^1\Pi_g$	Theory (Ref. [35])	9.41	23 227	53.53		$4s+3d$
	Present work	8.98	23 570	55.80	2255	
$3^1\Pi_g$	Expt. (Ref. [4])	8.75	26 433	66.04	2736	$4s+5p$
	Present work	8.66	26 316	66.16	2724	
$4^1\Pi_g$	Present work	8.62	28 041	63.52	2294	$4p+4p$
$5^1\Pi_g$	Expt. (Ref. [13])	8.52	28 480	71.03	3368	$4s+4d$
	Present work	8.49	28 359	71.10	3347	
$1^3\Pi_u$	Expt. (Ref. [5])	7.32	9912	91.54	7524	$4s+4p$
	Theory (Ref. [46])	7.39	9278	91.82	7485	
	Theory (Ref. [35])	7.54	9855	88.28		
	Present work	7.34	9827	94.80	7485	
$2^3\Pi_u$	Theory (Ref. [35])	8.52	21 999	59.46		$4s+3d$
	Present work	8.13	21 848	72.70	3977	
$3^3\Pi_u$	Present work	8.92	23 617	58.20	5423	$4s+5p$
$4^3\Pi_u$	Present work	8.33	26 492		3843	$4p+4p$
$5^3\Pi_u$	Present work	8.94	26 853	88.94	4853	$4s+4d$
$1^3\Pi_g$	Theory (Ref. [35])	9.28	17 612	48.97		$4s+4p$
	Present work	9.02	17 817		505	
$2^3\Pi_g$	Present work	9.64	21 550	55.52	4274	$4s+3d$
$3^3\Pi_g$	Present work	8.44	25 286	71.09	3754	$4s+5p$
$4^3\Pi_g$	Present work	8.58	28 048	56.83	2287	$4p+4p$
$5^3\Pi_g$	Present work	8.52	28 052	81.62	3634	$4s+4d$
$1^1\Delta_g$	Theory (Ref. [35])	7.94	19 524	72.10		$4s+3d$
	Present work	7.73	19 841	80.06	5984	
$2^1\Delta_g$	Present work	8.15	25 283	62.73	5052	$4p+4p$
$3^1\Delta_g$	Expt. (Ref. [4])	8.34	27 954	74.21	3899	$4s+4d$
	Present work	8.30	27 868	75.10	3838	
$1^1\Delta_u$	Theory (Ref. [35])	9.39	24 497	50.36		$4s+3d$
	Present work	8.77	24 685	58.22	1139	
$2^1\Delta_u$	Present work	8.61	27 559	65.67	4147	$4p+4p$

TABLE III. (Continued).

State	Determination	$R_e$ (units of $a_0$ )	$T_e$ ( $\text{cm}^{-1}$ )	$\omega_e$ ( $\text{cm}^{-1}$ )	$D_e$ ( $\text{cm}^{-1}$ )	Dissociation limit $\text{K}[nl]+\text{K}[n'l']$
$1^3\Delta_u$	Theory (Ref. [35])	9.51	24 331	49.08		$4s+3d$
	Present work	8.84	24 595	55.18	1230	
$2^3\Delta_u$	Present work	7.99	27 613		2722	$4p+4p$
$3^3\Delta_u$	Present work	8.62	29 109	66.34	2597	$4s+4d$
$1^3\Delta_g$	Theory (Ref. [35])	8.39	21 095	73.89		$4s+3d$
	Present work	7.95	20 871	78.90	4956	
$2^3\Delta_g$	Present work	8.26	25 912	75.30	5794	$4s+4d$
$1^3\Sigma_g^-$	Present work	7.55	26 813	66.64	3522	$4p+4p$

the  $4s$ ,  $4p$ ,  $3d$ , and  $4f$  experimental atomic energies [53] for K. As previously observed for Na [1], the energy of the  $4f$  atomic level appears insensitive to the choice of a corresponding cutoff radius, and we have taken it to be equal to  $\rho_\lambda^d$ . Finally, we obtain  $\rho_\lambda^l=2.067a_0$ ,  $\rho_\lambda^p=1.905a_0$ , and  $\rho^{d,f,\lambda}=1.960a_0$ . For a heteronuclear molecule, the core-polarization effects of each atom are different, and two sets of parameters must be defined. For NaK, we have therefore used the values obtained for potassium and those of sodium defined in Ref. [1].

With these data, we have computed atomic energies for the  $4s$  level up to  $5d$  for potassium. We obtain a good agreement with experimental data [53]. The discrepancies are less than  $10 \text{ cm}^{-1}$  for the lowest atomic levels, and less than  $50 \text{ cm}^{-1}$  for the most highly excited states. The difference between theoretical and experimental values for highly excited levels indicates that the present basis should be increased for their description. However, all molecular states correlating to asymptotes up to  $\text{K}[4s]+\text{K}[5d]$  and  $\text{Na}[3s]+\text{K}[5d]$  may be described with a good accuracy.

Hence, to check the accuracy of our basis sets and polarization potentials, we have determined the spectroscopic constants of the ground state of the  $\text{K}_2^+$  and  $\text{NaK}^+$  cations treated as one effective electron system. Results are given in Table II. Comparisons of theoretical calculations and experimental data are very consistent. Although the equilibrium distance is too short for  $\text{K}_2^+$ , as previously found for  $\text{Na}_2^+$ , we obtain an excellent agreement with other experimental values [54,55] especially for the dissociation energy. In both cases, comparisons with the theoretical results of Müller and Meyer [37] and those of Ref. [46] achieved by an open-shell coupled, cluster method are very good. As in Ref. [1], the energies of  $\text{K}_2$  and NaK states are determined by a full valence configuration-interaction (CI) procedure. For  $\text{K}_2$ , the molecular basis contains  $36\sigma$ ,  $48\pi$ ,  $28\delta$ , and  $8\phi$  orbitals, while this includes  $34\sigma$ ,  $46\pi$ ,  $26\delta$ , and  $8\phi$  orbitals for NaK.

### III. SHORT-RANGE RESULTS

Adiabatic potential curves have been computed, without including the spin-orbit coupling, up to the  $\text{K}[4s]+\text{K}[6s]$

and  $\text{Na}[3s]+\text{K}[5d]$  dissociation limits, from  $5a_0$  to  $70a_0$ . Moreover, relevant oscillator strengths for  $\text{K}_2$  and permanent dipole moments for NaK have been determined, and all data may be obtained upon request. In the first part of their analysis, we compare adiabatic potential curves with available experimental data.

#### A. Spectroscopic constants

Spectroscopic constants of  $\text{K}_2$  are presented in Table III, whereas they are reported in Table IV for NaK. For the two alkali dimers, the ground state is reproduced very well. The error in the equilibrium distance is equal to  $0.03a_0$  for  $\text{K}_2$  and  $0.04a_0$  for NaK, while those in the dissociation energy  $D_e$  are  $162$  and  $89 \text{ cm}^{-1}$ , respectively. Agreement between theoretical and experimental vibrational constants is also excellent. Moreover, our results are in good agreement with the previous theoretical calculations of Refs. [37] and [44]. We may note that the spectroscopic constants of the ground state of  $\text{K}_2$  are not determined with a very good accuracy by the open-shell cluster method [46]. This demonstrates in particular the difficulty in describing with accuracy correlation effects by all electron theoretical methods.

For the two molecules and for relevant electronic states, the equilibrium distances  $R_e$  are systematically predicted to be a little shorter than the experimental values. We generally find the dissociation energy  $D_e$  and the excitation energy  $T_e$  to be lower than the experimental data, and the errors do not exceed  $150 \text{ cm}^{-1}$ . However, for many excited states the errors are lower than those obtained for the ground state for the two molecules, and previous calculations of Refs. [35] and [36–45] have been improved remarkably. For example, with the improvement of the Gaussian basis set and with the inclusion of an  $l$ -dependent core-polarization potential, we may determine the spectroscopic constant of the  $3^3\Delta$  NaK electronic state which was calculated as dissociative in Ref. [45].

In the case of  $\text{K}_2$ , the  $2^1\Sigma_u^+$  electronic state correlated to  $\text{K}[4s]+\text{K}[5s]$  presents two minima located at  $R=9.27a_0$  and  $14a_0$ . In our work on  $\text{Na}_2$  [1], the same situation has been observed for the  $2^1\Sigma_u^+$  electronic state dissociating into

TABLE IV. The same as Table III, but for 58 electronic states of NaK.

State	Determination	$R_e$ (units of $a_0$ )	$T_e$ ( $\text{cm}^{-1}$ )	$\omega_e$ ( $\text{cm}^{-1}$ )	$D_e$ ( $\text{cm}^{-1}$ )	Dissociation limit Na[ $nl$ ]+K[ $n'l'$ ]
1 $^1\Sigma^+$	Expt. (Ref. [15])	6.61	0	124.01	5275	$3s+4s$
	Theory (Ref. [37])	6.64	0	123.80	5170	
	Theory (Ref. [45])	6.45	0	127.60	5491	
	Theory (Ref. [36])	6.41	0	132.00	5000	
	Present work	6.57	0	123.44	5187	
2 $^1\Sigma^+$	Expt. (Ref. [16])	7.93	12 137	81.25	6220	$3s+4p$
	Theory (Ref. [45])	7.68	12 011	86.20	6532	
	Theory (Ref. [36])	7.96	12 300	76.00	5888	
	Present work	7.90	12 089	81.00	6121	
3 $^1\Sigma^+$	Expt. (Ref. [17])	8.40	17 787	69.66	4455	$3p+4s$
	Theory (Ref. [45])	8.39	18 368	61.70	4104	
	Theory (Ref. [36])	8.35	18 200	77.00	4114	
	Present work	8.32	17 837	68.74	4317	
4 $^1\Sigma^+$	Theory (Ref. [45])	13.70	22 245		4309	$3s+5s$
	Present work	13.57	21 874	33.92	4331	
5 $^1\Sigma^+$	Theory (Ref. [45])	8.18	24 147	104.20	3279	$3s+3d$
	Present work	8.11	23 527	112.00	3195	
6 $^1\Sigma^+$	Present work	7.96	25 445	84.90	4492	$3s+5p$
	Present work	8.19	27 109	64.50	3837	
7 $^1\Sigma^+$	Present work	8.19	27 109	64.50	3837	$4s+4s$
	Present work	8.19	27 109	64.50	3837	
8 $^1\Sigma^+$	Present work	7.87	28 139	83.00	4465	$3s+4d$
	Present work	7.87	28 139	83.00	4465	
9 $^1\Sigma^+$	Present work	7.67	28 562	96.20	4077	$3s+6s$
	Present work	7.67	28 562	96.20	4077	
10 $^1\Sigma^+$	Present work	7.75	29 527	84.00	3834	$3s+4f$
	Present work	7.75	29 527	84.00	3834	
11 $^1\Sigma^+$	Present work	7.88	30 391	80.60	3847	$3s+6p$
	Present work	7.88	30 391	80.60	3847	
12 $^1\Sigma^+$	Present work	7.74	30 869	87.00	3491	$3d+4s$
	Present work	7.74	30 869	87.00	3491	
13 $^1\Sigma^+$	Present work	7.64	31 101	82.20	4076	$3p+4p$
	Present work	7.64	31 101	82.20	4076	
14 $^1\Sigma^+$	Present work	7.69	31 166	94.80	4011	$3p+4p$
	Present work	7.69	31 166	94.80	4011	
1 $^3\Sigma^+$	Expt. (Ref. [15])	10.28	5066	22.99	209	$3s+4s$
	Theory (Ref. [45])	9.79	5200	26.90	291	
	Theory (Ref. [36])	10.56	4800	23.00	161	
	Present work	10.30	4990	22.65	197	
	Present work	10.30	4990	22.65	197	
2 $^3\Sigma^+$	Expt. (Ref. [18])		15 719	75.50	2580	$3s+4p$
	Expt. (Ref. [19])	7.75	15 998	73.79	2300	
	Expt. (Ref. [20])	8.05	16 283	68.64	2015	
	Theory (Ref. [45])	8.01	15 799	74.00	2645	
	Theory (Ref. [36])	8.20	16 100	77.00	2097	
	Present work	8.14	15 669	73.40	2541	
3 $^3\Sigma^+$	Theory (Ref. [45])	7.26	21 690	88.30	782	$3p+4s$
	Present work	7.44	21 380	94.20	774	

TABLE IV. (Continued).

State	Determination	$R_e$ (units of $a_0$ )	$T_e$ ( $\text{cm}^{-1}$ )	$\omega_e$ ( $\text{cm}^{-1}$ )	$D_e$ ( $\text{cm}^{-1}$ )	Dissociation limit Na[ $nl$ ]+K[ $n'l'$ ]
$4^3\Sigma^+$	Theory (Ref. [45])	7.83	23 649	70.90	2282	$3s+5s$
	Present work	7.96	23 850	74.00	2355	
$5^3\Sigma^+$	Theory (Ref. [45])	9.89	25 381	73.70	2047	$3s+3d$
	Present work	9.81	24 868	97.00	1855	
$6^3\Sigma^+$	Theory (Ref. [45])	9.89	25 381	73.70	2047	$3s+5p$
	Present work	9.81	24 868	97.00	1855	
$7^3\Sigma^+$	Theory (Ref. [45])	9.89	25 381	73.70	2047	$4s+4s$
	Present work	8.35	26 681	110.00	3256	
$8^3\Sigma^+$	Theory (Ref. [45])	9.89	25 381	73.70	2047	$3s+4d$
	Present work	8.49	27 588	106.00	3359	
$9^3\Sigma^+$	Theory (Ref. [45])	9.89	25 381	73.70	2047	$3s+6s$
	Present work	7.81	28 212	166.00	4392	
$10^3\Sigma^+$	Theory (Ref. [45])	9.89	25 381	73.70	2047	$3s+4f$
	Present work	7.74	29 131	92.00	3508	
$11^3\Sigma^+$	Theory (Ref. [45])	9.89	25 381	73.70	2047	$3s+6p$
	Present work	7.65	30 072	92.00	3289	
$12^3\Sigma^+$	Theory (Ref. [45])	9.89	25 381	73.70	2047	$3d+4s$
	Present work	7.76	30 540	90.00	3698	
$13^3\Sigma^+$	Theory (Ref. [45])	9.89	25 381	73.70	2047	$3p+4p$
	Present work	7.61	30 989	93.00	3371	
$14^3\Sigma^+$	Theory (Ref. [45])	9.89	25 381	73.70	2047	$3p+4p$
	Present work	7.75	31 152	86.00	4025	
$1^1\Pi$	Present work	7.67	31 821	89.90	3356	$3s+4p$
	Expt. (Ref. [21])	7.59	16 993	71.50	1306	
	Expt. (Ref. [22])	7.58	16 993	71.43	1306	
	Expt. (Ref. [23])	7.58	16 993	71.46	1305	
	Theory (Ref. [45])	7.69	17 365	61.30	1079	
	Theory (Ref. [36])	7.69	17 500	65.00	726	
	Present work	7.63	17 016	67.60	1193	
$2^1\Pi$	Expt. (Ref. [24])	7.92	20 093	81.52	2149	$3p+4s$
	Theory (Ref. [45])	7.58	20 643	84.00	1839	
	Theory (Ref. [36])	7.69	21 000	71.00	1291	
	Present work	7.81	20 082	83.00	2072	
$3^1\Pi$	Theory (Ref. [45])	9.05	26 690	46.00	738	$3s+3d$
	Present work	8.52	25 568	47.20	1155	
$4^1\Pi$	Theory (Ref. [45])	9.05	26 690	46.00	738	$3s+5p$
	Present work	8.52	25 568	47.20	1155	
$5^1\Pi$	Theory (Ref. [45])	9.05	26 690	46.00	738	$3s+4d$
	Present work	7.87	26 394	87.90	3544	
$6^1\Pi$	Theory (Ref. [45])	9.05	26 690	46.00	738	$3s+4f$
	Present work	7.74	27 659	84.40	4945	
$7^1\Pi$	Theory (Ref. [45])	9.05	26 690	46.00	738	$3s+6p$
	Present work	7.81	29 286	82.70	4075	
$8^1\Pi$	Theory (Ref. [45])	9.05	26 690	46.00	738	$3d+4s$
	Present work	7.77	29 756	81.40	4482	
$9^1\Pi$	Theory (Ref. [45])	9.05	26 690	46.00	738	$3p+4p$
	Present work	7.72	30 609	86.50	3751	
$10^1\Pi$	Theory (Ref. [45])	9.05	26 690	46.00	738	$3p+4p$
	Present work	7.74	31 163	87.00	4013	
$10^1\Pi$	Theory (Ref. [45])	9.05	26 690	46.00	738	$3p+4p$
	Present work	7.73	31 357	88.00	3820	



TABLE IV. (Continued).

State	Determination	$R_e$ (units of $a_0$ )	$T_e$ ( $\text{cm}^{-1}$ )	$\omega_e$ ( $\text{cm}^{-1}$ )	$D_e$ ( $\text{cm}^{-1}$ )	Dissociation limit $\text{Na}[nl] + \text{K}[n'l']$
1 $^1\Delta$	Theory (Ref. [45])	7.04	23 352	103.60	4076	$3s + 3d$
	Present work	7.17	22 961	96.60	3761	
2 $^1\Delta$	Theory (Ref. [45])	7.90	29 905	72.80	4744	$3s + 4d$
	Present work	7.76	28 080	85.50	4524	
3 $^1\Delta$	Theory (Ref. [45])	9.51	35 492	50.60	2089	$3s + 4f$
	Present work	7.43	28 332	98.00	5029	
4 $^1\Delta$	Theory (Ref. [45])	9.51	35 492	50.60	2089	$3d + 4s$
	Present work	7.56	30 883	74.00	3477	
5 $^1\Delta$	Theory (Ref. [45])	9.51	35 492	50.60	2089	$3p + 4p$
	Present work	7.66	30 920	103.00	4257	
1 $^3\Pi$	Expt. (Ref. [25])	6.62	11 562	120.41	6737	$3s + 4p$
	Theory (Ref. [45])	6.50	11 534	122.20	6910	
	Theory (Ref. [36])	6.52	11 900	129.00	6291	
	Present work	6.54	11 508	121.71	6702	
2 $^3\Pi$	Expt. (Ref. [26])	7.98	20 248	67.38	2012	$3p + 4s$
	Theory (Ref. [45])	7.84	20 508	69.30	1964	
	Theory (Ref. [36])	8.43	21 200	69.00	1049	
	Present work	8.00	20 190	67.09	1964	
3 $^3\Pi$	Theory (Ref. [45])	10.50	25 099	51.70	2329	$3s + 3d$
	Present work	7.39	25 165	101.00	1558	
4 $^3\Pi$	Theory (Ref. [45])	10.50	25 099	51.70	2329	$3s + 5p$
	Present work	8.24	25 718	165.00	4219	
5 $^3\Pi$	Theory (Ref. [45])	10.50	25 099	51.70	2329	$3s + 4d$
	Present work	8.09	27 224	69.20	5380	
6 $^3\Pi$	Theory (Ref. [45])	10.50	25 099	51.70	2329	$3s + 4f$
	Present work	7.64	27 966	90.70	5395	
7 $^3\Pi$	Theory (Ref. [45])	10.50	25 099	51.70	2329	$3s + 6p$
	Present work	7.53	29 548	93.90	4691	
8 $^3\Pi$	Theory (Ref. [45])	10.50	25 099	51.70	2329	$3d + 4s$
	Present work	8.08	30 323	41.00	4037	
9 $^3\Pi$	Theory (Ref. [45])	10.50	25 099	51.70	2329	$3p + 4p$
	Present work	7.64	30 857	90.00	4320	
10 $^3\Pi$	Theory (Ref. [45])	10.50	25 099	51.70	2329	$3p + 4p$
	Present work	7.75	31 160	88.00	4017	
1 $^3\Delta$	Theory (Ref. [45])	7.17	24 296	97.70	3132	$3s + 3d$
	Present work	7.35	23 647	93.60	3075	
2 $^3\Delta$	Theory (Ref. [45])	7.77	29 982	81.30	4667	$3s + 4d$
	Present work	7.74	28 067	85.90	4537	
3 $^3\Delta$	Theory (Ref. [45])	dissociative				$3s + 4f$
	Present work	7.53	28 834	92.70	4527	
4 $^3\Delta$	Theory (Ref. [45])	dissociative				$3d + 4s$
	Present work	7.70	30 885	87.50	3476	
5 $^3\Delta$	Theory (Ref. [45])	dissociative				$3p + 4p$
	Present work	7.60	31 298	89.00	3879	

TABLE V. Estimated deviations from experimental values for spectroscopic constants of the  $K_2$  and NaK molecules for various calculations. (Average deviations over 17 electronic states for  $K_2$  and over nine states for NaK.)

	$\Delta R_e$ (units of $a_0$ )	$\Delta T_e$ ( $\text{cm}^{-1}$ )	$\Delta \omega_e$ ( $\text{cm}^{-1}$ )	$\Delta D_e$ ( $\text{cm}^{-1}$ )
$K_2$				
Theory (Ref. [35])	0.32	234	5.52	
Present work	0.05	111	1.78	84
$NaK$				
Theory (Ref. [45])	0.20	266	4.19	198
Theory (Ref. [36])	0.18	491	5.48	481
Present work	0.05	46	1.24	72

$Na[3s]+Na[4s]$ , and Cooper *et al.* [56] have shown that this pattern was typical of an ionic-covalent interaction. Using previous studies on different alkali dimers [56–58], Kowalczyk, Katern, and Engelke [6] suggested that this state has a double-well structure due to an avoided crossing between two diabatic states, one being a Rydberg state correlated to  $K[4s]+K[5s]$ , the other being ionic at large internuclear distance. Unfortunately, their experiments were insufficient to determine with accuracy the corresponding potential curve and, in particular, if it was characterized by one or two minima. Nevertheless, from their measurements they deduced some spectroscopic constants. According to a comparison of our results with experimental values, we suggest that Kowalczyk, Katern, and Engelke observed the second (outer) minimum. In Sec. IV will show that this results effectively from an interaction between ionic and covalent states.

Recently, some experiments were devoted to highly excited states [4,7,11,13] dissociating into the asymptotes close to  $K[4p]+K[4p]$ . We obtained a very good agreement with experiments for spectroscopic constants of the  $5^1\Sigma_g^+$ ,  $6^1\Sigma_g^+$ ,  $9^1\Sigma_g^+$ ,  $3^1\Delta_g$ ,  $3^1\Pi_u$ ,  $4^1\Pi_u$ , and  $3^1\Sigma_u^+$  molecular states. Except for the  $3^1\Sigma_u^+$  and  $3^1\Pi_u$  states, where the errors in the excitation energy for the first state and on the equilibrium distance for the second are more important, the errors in the excitation and dissociation energies do not exceed  $100\text{ cm}^{-1}$ , and those in the equilibrium distance do not exceed  $0.1a_0$ . Only the agreement between vibrational constants is less satisfying. Moreover, we may observe that our data on the  $5^1\Pi_g$  molecular state correlated to  $K[4s]+K[4d]$  are in good agreement with experimental values for a  $1^1\Pi_g$  state [13], thought to be diabatically dissociating into  $K[4s]+K[5d]$ . The equilibrium distances  $R_e$  differ by  $0.03a_0$ , and the vibrational constants  $w_e$  by  $0.07\text{ cm}^{-1}$ , while the difference for the excitation energy  $T_e$  is equal to  $121\text{ cm}^{-1}$ . Thus we finally suggest that the dissociation limit of this experimental state corresponds to  $K[4s]+K[4d]$ . Recent highly excited  $1^1\Delta_g$  states correlated to  $K[4s]+K[6d]$ , for example, have been observed [14], but unfortunately we cannot compare our results with them.

For NaK, the agreement with experiment is often excellent except for the  $2^3\Sigma^+$  molecular state correlated to  $Na[3p]+K[4s]$ . However, the agreement between all theoretical calculations [36–45] is very good. Although many experimental works have been devoted to this state [18–20], it is difficult to compare our results with the various experimental spectroscopic constants. Recently, Kowalczyk, Der-

ouard, and Sadeghi [27] determined with accuracy the number of vibrational levels and their position. They compared with other experimental determinations and concluded that the most accurate spectroscopic constants were those of Kowalczyk [19]. They showed in particular that this state is very perturbed by the  $1^1\Pi$  and  $1^3\Pi$  electronic states (see below), and suggested that these data could be improved. Nevertheless if we compare our values with the various experimental ones, we may suggest that Derouard and Sadeghi [18] have reported the most accurate spectroscopic constants.

Our present results are in overall very good agreement with available experimental values. In Table V we present the estimated errors in the spectroscopic constants for previous and present theoretical works. The averaged value of the deviation between experimental and theoretical determinations has been computed for 17 states of  $K_2$  and nine states of NaK. In both cases, our theoretical results show remarkable improvement compared to previous theory, and we again obtain the accuracy of our previous calculations on  $Na_2$  [1] and those on  $Cs_2$  and  $Rb_2$  [38]. Moreover, for NaK we determined to check the accuracy of our wave functions, and the variation of the permanent dipole moment of each state versus the internuclear distance. In the case of the ground state, at the equilibrium distance we find a permanent dipole moment equal to 2.758 D, which is in good agreement with the experimental value [59], ( $\mu[R_e]=2.733(2)\text{ D}$ ) and with the prior theoretical value of Müller and Meyer [37] ( $\mu[R_e]=2.735\text{ D}$ ). Thus we may finally conclude that accurate results may be obtained when core-polarization effects are represented by an effective potential including  $l$ -dependent cutoff parameters, and that the pseudopotential method [38] is well adapted to the description of homonuclear and heteronuclear alkali dimers.

## B. Comparison with RKR curves

When potential curves deduced from experiments are available, we can check in detail the accuracy of our calculations. We have chosen in particular to compare our results with those known at intermediate and large internuclear distances. Potential curves of the ground state of the two molecules are compared in Figs. 1 and 2 with experimental data of Amiot [2] for  $K_2$  and with those of Ross *et al.* [15] for NaK. In both cases, the agreement is excellent, in particular for intermediate distances, the difference being equal to  $4\text{ cm}^{-1}$  at  $R=17a_0$  for  $K_2$ , and to  $3.5\text{ cm}^{-1}$  at  $R=15a_0$  for NaK.

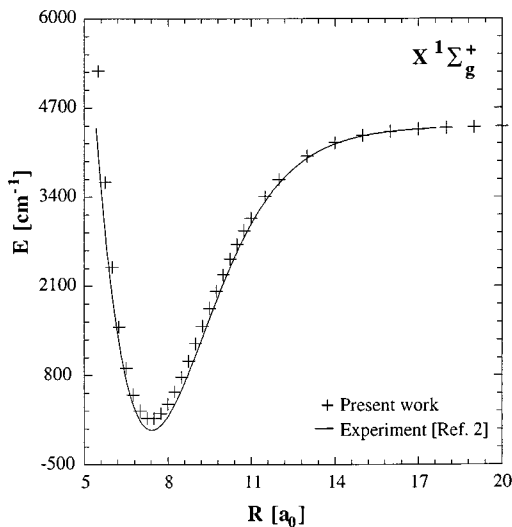


FIG. 1. Ground state of the  $K_2$  molecule: comparison of the computed curve with the experimental curve of Ref. [2].

Comparison with experiment is also very good for the lowest excited states. In Fig. 3 we present our results for the  $1^1\Pi_g$  state correlated to  $K[4s] + K[4p]$ . Our calculations are very comparable with the experimental values of Ref. [12], and the long-range potential curve is reproduced with an accuracy of  $10 \text{ cm}^{-1}$  up to  $30a_0$ . Two other potential curves dissociating into  $K[4s] + K[4p]$  are compared in Fig. 4 to recent determinations of Ref. [5]. The comparison is very consistent, and the position of the crossing between the  $1^3\Pi_u$  and  $1^1\Sigma_u^+$  states is reproduced with a precision of  $0.04a_0$ . We find it at  $R_c = 8.94a_0$  with an energy of  $11\,260 \text{ cm}^{-1}$ , while the experimental crossing is located at  $R_c = 8.98a_0$  with  $E = 11\,165 \text{ cm}^{-1}$ .

For NaK, the present calculations are also very accurate. Potential curves of the  $1^3\Pi$ ,  $1^1\Pi$ , and  $2^3\Sigma^+$  electronic states correlated to  $Na[3s] + K[4p]$  are displayed in Fig. 5

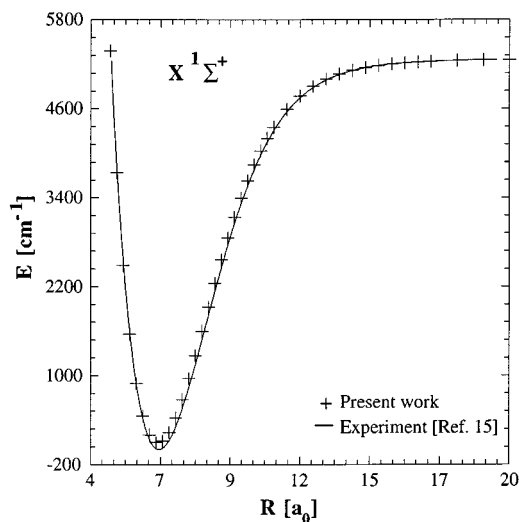


FIG. 2. Ground state of the NaK molecule: comparison of the computed curve with the experimental curve of Ref. [15].

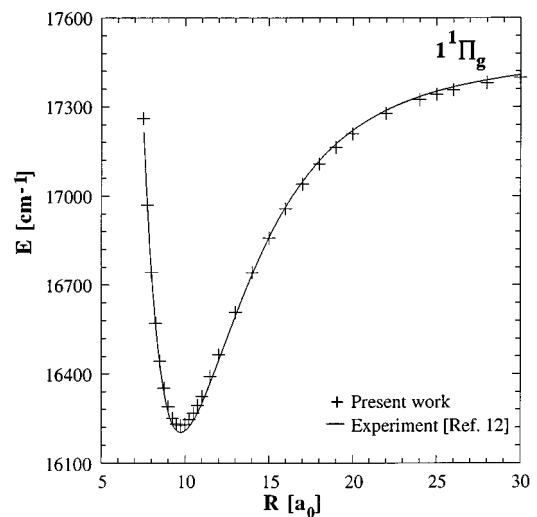


FIG. 3. Lowest excited states of  $K_2$ : comparison of the computed curve with the experimental curve of Ref. [12] for the  $1^1\Pi_g$  state correlated to  $K[4s] + K[4p]$ .

from  $5a_0$  to  $20a_0$ . Comparison with Refs. [21] and [25] is very good, and as in Refs. [19] and [27] we may note that the  $2^3\Sigma^+$  state is strongly perturbed by the  $1^1\Pi$  state at short distances, but also by the  $1^3\Pi$  state at intermediate internuclear distances. We observe a crossing between the  $2^3\Sigma^+$  and  $1^3\Pi$  states located at  $R_c = 10.95a_0$ . These perturbations may explain the differences between various experimental spectroscopic constants.

Although comparison with experimental potential curves is excellent for the lowest states for both molecules, the major part of the present results, mainly for highly excited states, corresponds to predictions. In order to confirm or invalidate them, further experimental investigations would be very interesting. In the remainder of this paper, we now pay particular attention to adiabatic potential curves for which

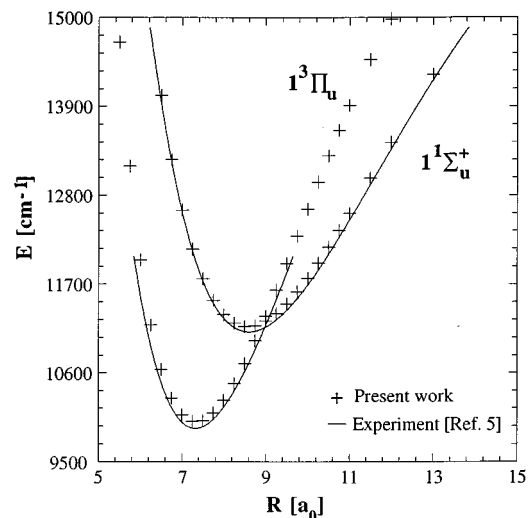


FIG. 4. Lowest excited states of  $K_2$ : comparison of the computed curve with the experimental curve of Ref. [5] for the  $1^3\Pi_u$  and  $1^1\Sigma_u^+$  states correlated to  $K[4s] + K[4p]$ .

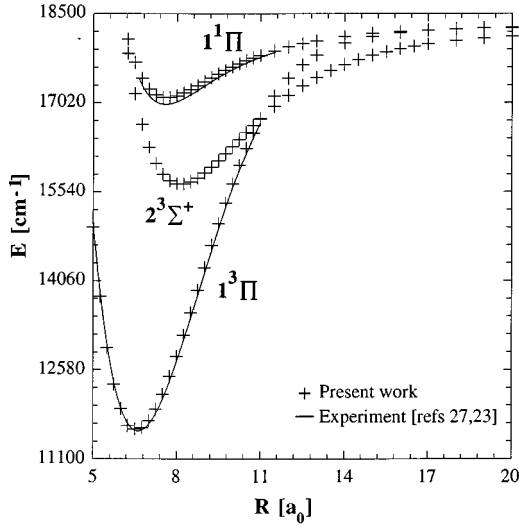


FIG. 5. Lowest excited states of the NaK molecule dissociating into  $\text{Na}[3s] + \text{K}[4p]$ : comparison of the computed curves with the experimental curves of Refs. [21] and [25] for the  $1^1\Pi$  and  $1^3\Pi$  states. The  $2^3\Sigma^+$  state is strongly perturbed by these two states (at short distance by the  $1^1\Pi$  state and at intermediate internuclear distances by the  $1^3\Pi$  state).

interesting structures are displayed at large interatomic separation.

#### IV. STRUCTURES IN LONG-RANGE POTENTIAL CURVES OF HIGHLY EXCITED STATES

As in the case of  $\text{Na}_2$  [43], numerous avoided crossings and wells are located in the adiabatic potential curves of  $1^3\Sigma^+$  and  $3\Pi$  symmetries, at very large internuclear distances. The position and the depth of the minima are reported in Table VI. For  $\text{K}_2$ , we predict six wells in adiabatic potential curves of molecular states correlated to the asymptotes close to  $\text{K}[4p] + \text{K}[4p]$ . We find, in particular, one well in the potential curves of  $5^1\Sigma_g^+$  and  $4^1\Sigma_u^+$  states correlated to

TABLE VI. Position (in  $a_0$ ) and depth (in  $\text{cm}^{-1}$ ) of wells located at large internuclear distances for the  $1^3\Sigma^+$  and  $3\Pi$  symmetries.

Molecular state	Position (units of $a_0$ )	Depth ( $\text{cm}^{-1}$ )
$\text{K}_2$		
$5^1\Sigma_g^+ [4s+4p]$	22.00	2651
$6^1\Sigma_g^+ [4p+4p]$	32.00	1187
$4^1\Sigma_u^+ [4s+4p]$	22.80	2652
$5^1\Sigma_u^+ [4s+4d]$	32.60	2560
$5^3\Pi_u [4s+4d]$	19.75	1396
$5^3\Pi_g [4s+4d]$	21.20	1234
$\text{NaK}$		
$4^1\Sigma^+ [3s+5s]$	14.00	4334
$6^1\Sigma^+ [3s+5p]$	23.10	2854
$12^1\Sigma^+ [3d+4s]$	25.90	723
$14^1\Sigma^+ [3p+4p]$	26.80	621
$8^3\Sigma^+ [3s+4d]$	15.30	1320
$9^3\Pi [3p+4p]$	25.10	652

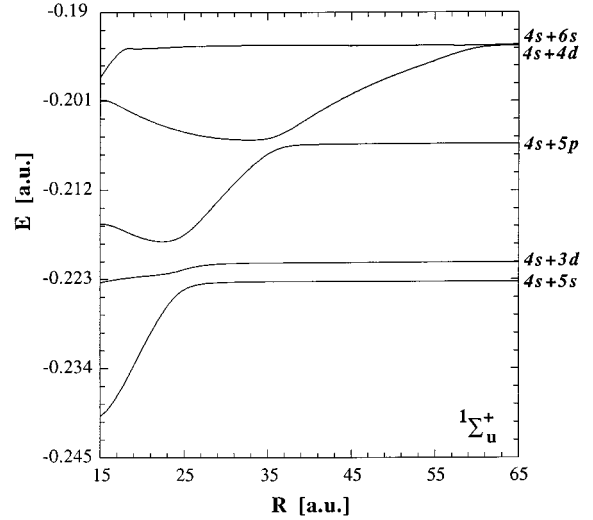


FIG. 6. Long-range adiabatic computed potential curves of the  $\text{K}_2$  molecule for the  $1^1\Sigma_u^+$  electronic states correlated to asymptotes from  $\text{K}[4s] + \text{K}[5s]$  up to  $\text{K}[4s] + \text{K}[6s]$ .

$\text{K}[4s] + \text{K}[5p]$ . These minima present the same characteristics, their position and their depth being respectively  $R=22a_0$  and  $E=2651 \text{ cm}^{-1}$  for  $5^1\Sigma_g^+$  and  $R=22.80a_0$  and  $E=2652 \text{ cm}^{-1}$  for  $4^1\Sigma_u^+$ . For  $\text{Na}_2$  [43], we have demonstrated that the occurrence of structures at large internuclear separation was due to pseudocrossings between ionic and covalent states, the ionic state being correlated, respectively, to  $\text{Na}^+ + \text{Na}^- [1S]$  and  $\text{Na}^+ + \text{Na}^- [3P_0]$  for the  $1^1\Sigma^+$  and  $3\Pi$  symmetries. In our case, the minima of the  $5^1\Sigma_g^+$  and  $4^1\Sigma_u^+$  adiabatic potential curves correspond to a pseudocrossing between the ionic state correlated to  $\text{K}^+ + \text{K}^- [1S]$  and the  $1^1\Sigma_{g,u}^+$  covalent states dissociating into  $\text{K}[4s] + \text{K}[5p]$ , which occurs at the same internuclear distance in relevant adiabatic potential curves. Similar comments may be also made for the  $5^3\Pi_g$  and  $5^3\Pi_u$  states correlated to  $\text{K}[4p] + \text{K}[4p]$ .

In the case of NaK, we also predict six minima and, for the first time to our knowledge, one of  $3\Sigma^+$  symmetry. To illustrate them, we have chosen to display, in Figs. 6–8, long-range adiabatic potential curves of  $1^1\Sigma_u^+$  highly excited states correlated to asymptotes from  $4s+5s$  up to  $4s+6s$  for  $\text{K}_2$ , and those of the  $1^1\Sigma^+$  and  $3\Sigma^+$  excited states dissociating, respectively, to asymptotes from  $3s+5s$  up to  $3s+4f$  and from  $3s+5p$  up to  $3p+4p$  for NaK. Numerous avoided crossings are present, and we now propose to explain them.

In previous work [43] we developed, to interpret them, a diabatic procedure in which we extracted, from pseudopotential calculations, a set of covalent and ionic curves and corresponding couplings. Applying this method for  $\text{K}_2$ , we identified two ionic states responsible for these patterns. The first one is correlated to the  $\text{K}^+ + \text{K}^- [1S]$  limit, and has an energy of  $-0.495 \text{ eV}$  in comparison with the  $\text{K} + \text{K}^+$  limit. The value  $0.495 \text{ eV}$ , corresponding to the electronic affinity of the potassium atom, is in good agreement with the experimental data of Ref. [60] ( $E.A. = 0.501 \text{ eV}$ ). The second ionic state is an autoionizing state dissociating into  $\text{K}^+ + \text{K}^- [3P_0]$ .

We display diabatic  $1^1\Sigma_u^+$  potential curves in Fig. 9. We note that the positions of crossings between diabatic covalent curves and the ionic curve are very close to those of different structures occurring in relevant adiabatic potential curves. In

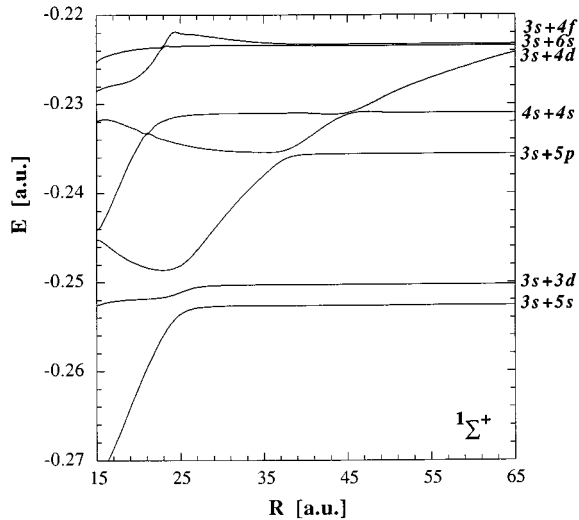


FIG. 7. Long-range adiabatic computed potential curves of the NaK molecule for the  $1\Sigma^+$  electronic states correlated to asymptotes from Na[3s]+K[5s] up to Na[3s]+K[4f].

particular, the crossing between the  $2^1\Sigma_u^+$  covalent curve and the  $K^+ + K^- [1S]$  ionic curve is located at  $R_c = 21.80a_0$  and corresponds at the end of the second well of the adiabatic  $2^1\Sigma_u^+$  state correlated to K[4s]+K[5s]. Then, from an analysis of diabatic pseudopotential results, we may confirm the existence of two minima in the adiabatic  $2^1\Sigma_u^+$  potential curve and, in particular, the ionic character of the second (outer) well.

For the NaK molecule, the situation is more complicated, since we must take into account two ionic asymptotes  $Na^- [1S] + K^+$  and  $Na^+ + K^- [1S]$  separated by 0.84 eV. There are important perturbations in the adiabatic potential curves, and we propose to explain some of the structures observed in the  $1\Sigma^+$  and  $3\Sigma^+$  symmetries by analyzing the variation of the permanent dipole moment.

In Fig. 10, we report permanent dipole moments versus the internuclear distance for the  $4^1\Sigma^+$  to  $8^1\Sigma^+$  states. Strong

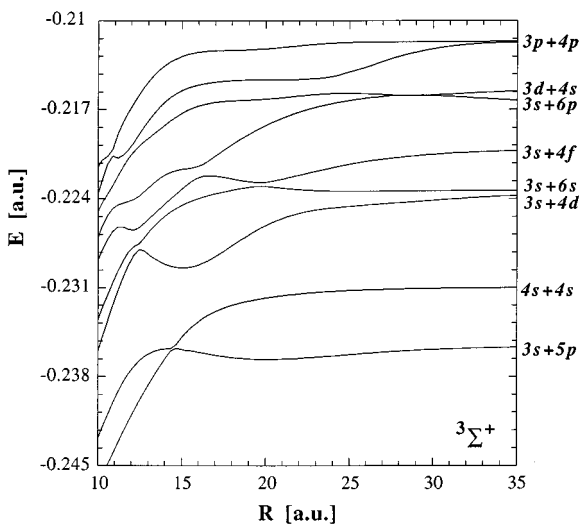


FIG. 8. Same as Fig. 7 but for  $3\Sigma^+$  electronic states dissociating to asymptotes from Na[3s]+K[5p] up to Na[3p]+K[4p].

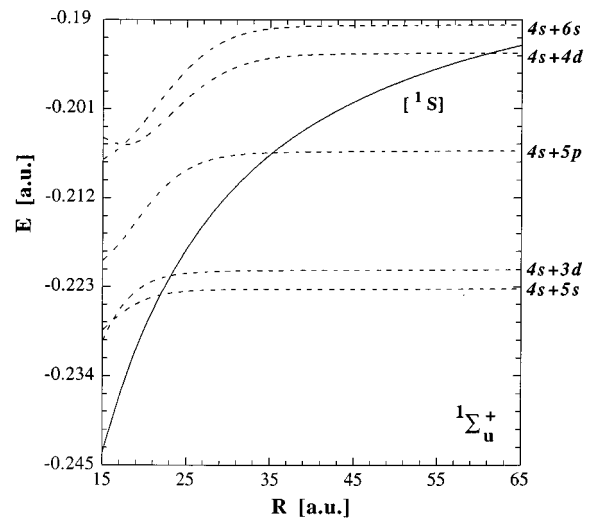


FIG. 9. Diabatic potential curves correlated to asymptotes from K[4s]+K[5s] up to K[4s]+K[6s] for the  $1\Sigma_u^+$  states. (Broken lines: covalent states; full lines: ionic states correlated to  $K^+ + K^- [1S]$ ).

variations are observed at  $R > 25a_0$  mainly for the  $6^1\Sigma^+$ ,  $7^1\Sigma^+$ , and  $8^1\Sigma^+$  states. They may be interpreted as a movement of the electronic charge from one core  $Na^+$  or  $K^+$  to the other one. When the charge transfer is complete, the permanent dipole moment of the molecular state is practically equal to the ionic value of  $Na^+K^-$  or  $Na^-K^+$  (equal to  $\mu[D] = +2.5418029R$  [a.u.], minus sign for  $Na^+K^-$  and plus sign for  $Na^-K^+$ ). This situation is clearly observed for  $8^1\Sigma^+$  for internuclear distances in the range of  $45a_0$  and  $65a_0$ , but also for the  $6^1\Sigma^+$  and  $7^1\Sigma^+$  states for smaller values of  $R$ , where the charge transfer is provided from  $K^+$  to  $Na^-$ . So we may conclude that in these various ranges of interatomic separation, the adiabatic potential curves of these states have an ionic pattern. Moreover, we may check this conclusion by determining the position of the crossings between the ionic and covalent potential curves. The energy of the ionic state

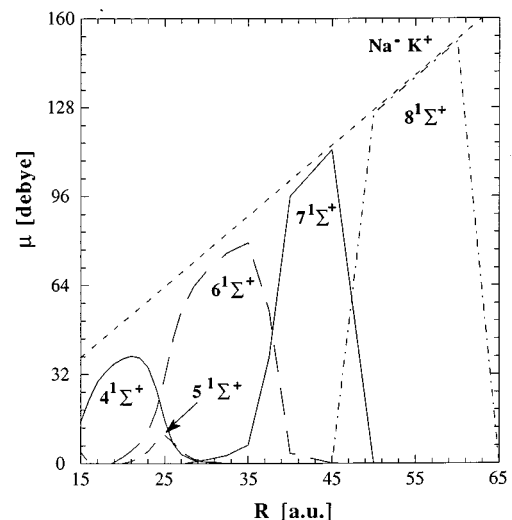


FIG. 10. Variation of the permanent dipole moment  $\mu$  of the  $4^1\Sigma^+$  to  $8^1\Sigma^+$  states correlated to asymptotes from Na[3s]+K[4d] up to Na[3s]+K[5p] versus the internuclear distance.

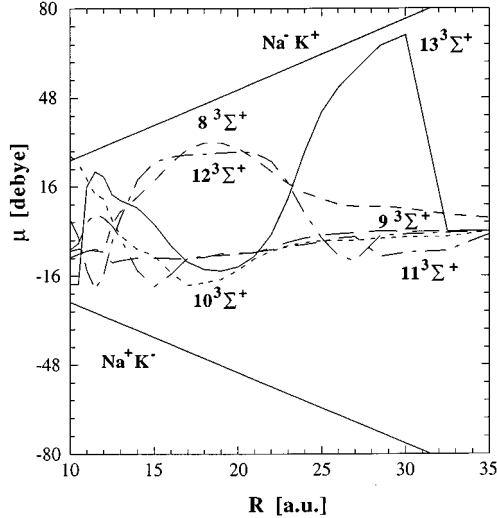


FIG. 11. Same as Fig. 10 but for the 8 to 13  $^3\Sigma^+$  states correlated to asymptotes from  $\text{Na}[3s] + \text{K}[4d]$  up to  $\text{Na}[3p] + \text{K}[4p]$ .

versus interatomic separation is written as

$$E_{\text{ionic}}(R) = E_{\text{ionic}}(\infty) - \frac{1}{R} - \frac{\alpha}{2R^4} \quad (6)$$

where  $\alpha$  is the polarizability of the negative ion.

At large internuclear distance,  $-\alpha/2R^4$  becomes negligible, and the position  $R_n$  of a crossing may be finally approximated by

$$R_n = \frac{1}{E_{\text{ionic}}(\infty) - E_n}, \quad (7)$$

where  $E_n$  is the energy of covalent dissociation limit.

In the case of  $6^1\Sigma^+$ , we obtain  $R_n = 37.33a_0$ . This is included in the range of internuclear distances where the values of the  $6^1\Sigma^+$  permanent dipole moment are very close to that of  $\text{Na}^-\text{K}^+$ . For the  $8^1\Sigma^+$  state, we find  $R_n = 68.33a_0$ , which shows that the relevant potential curve may be considered as ionic for internuclear distances varying from  $45a_0$  to  $65a_0$ . Moreover, as soon as the relevant permanent dipole moment decreases, the value of the  $7^1\Sigma^+$  dipole moment increases and becomes ionic for  $35a_0 < R < 50a_0$  before decreasing to zero. We may note that the  $5^1\Sigma^+$  permanent dipole moment stays practically equal to zero, except at  $R = 25a_0$  where we observe a small variation. If we examine corresponding adiabatic potential curves, we find at  $R = 25a_0$  an avoided crossing between the  $4^1\Sigma^+$ ,  $5^1\Sigma^+$ , and  $6^1\Sigma^+$  states, which does not modify the  $5^1\Sigma^+$  potential curve. Then, as variations of the permanent dipole moments of  $4^1\Sigma^+$  and  $6^1\Sigma^+$  are ionic, respectively, just before and after this interatomic separation, we may consider that the  $5^1\Sigma^+$  permanent dipole moment is finally ionic at  $R = 25a_0$ . Nevertheless, additional calculations should be provided to discuss in detail the modifications of the permanent dipole moment.

In Fig. 11, we report permanent dipole moments versus the internuclear distance for the  $8^3\Sigma^+$  to  $13^3\Sigma^+$  states. The permanent dipole moment of the  $13^3\Sigma^+$  state is clearly ionic for  $25a_0 < R < 30a_0$ , and presumably also for those of the

$8^3\Sigma^+$  and  $12^3\Sigma^+$  states for internuclear distances included between  $13a_0$  and  $25a_0$ . As the situation is more complicated than for the  $1^1\Sigma^+$  symmetry, we suggest that the well observed in the  $8^3\Sigma^+$  adiabatic potential curve is due to an ionic-covalent interaction. To confirm this remark and to identify the ionic state, diabatic calculations should be performed.

These patterns for the  $\text{Li}_2$ ,  $\text{Cs}_2$ , and  $\text{Rb}_2$  alkali dimers have previously been predicted only for  $1^1\Sigma^+$  symmetry, to the best of our knowledge [38,58]. As for  $\text{Na}_2$ , our work demonstrates the presence of structures resulting from an excited ionic curve of  $3\Pi$  symmetry. For the first time, to our knowledge, we identify an ionic state in the  $3^3\Sigma^+$  potential curves, and suggest that an autoionizing ionic state correlated to  $\text{Na}^-\text{K}^+$  is responsible for their numerous perturbations, this one being correlated to the  $\text{Na}^-[3S] + \text{K}^+$  or  $\text{Na}^-[3P_0] + \text{K}^+$  asymptotes.

## V. CONCLUSION

In this paper, we presented spectroscopic constants for the ground state and 60 excited states for  $\text{K}_2$ , 57 in the case of  $\text{NaK}$ , and relevant potential-energy curves over a wide range of internuclear distances. By comparison with available experimental data, we have discussed the accuracy of our calculations. A very good agreement with experimental determinations is obtained for the lowest excited state as well as for highly excited states correlated to the  $\text{K}[4p] + \text{K}[4p]$  and  $\text{K}[4s] + \text{K}[6s]$  asymptotes. It should now be very interesting to follow the analysis of our results on the first excited states by comparing them with long-range calculations, and this comparison will be reported in a forthcoming paper.

Important structures have been observed in the  $1^3\Sigma^+$  and  $3\Pi$  adiabatic potential curves of highly excited states. In the case of the  $1^1\Sigma^+$  and  $3\Pi$  symmetries, the ionic curves responsible for such structures are correlated, respectively, to  $\text{K}^+ + \text{K}^-[1S]$  and  $\text{K}^+ + \text{K}^-[3P_0]$  for  $\text{K}_2$ , and to  $\text{Na}^-[1S] + \text{K}^+$  and  $\text{Na}^-[3P_0] + \text{K}^+$  for  $\text{NaK}$ . For  $3^3\Sigma^+$  symmetry, we may assume for  $\text{NaK}$  that the ionic state corresponds to the  $\text{Na}^-[3S] + \text{K}^+$  or  $\text{Na}^-[3P_0] + \text{K}^+$  resonances.

Nevertheless the present results constitute a strong start for theoretical studies of collisional processes. In a recent work on  $\text{Na}_2$  [61], using a multichannel Landau-Zener model we estimated the dynamical effects of all avoided crossings present in adiabatic excited potential curves. We established that the structures located at large interatomic separation played a major role in the dynamics of atom-atom collisions at low energy. Furthermore, with the improvement of other previous calculations [31,32], we recently showed that, as well as the  $3^3\Sigma_u^+$  state, four other molecular channels ( $3^1\Pi_u$ ,  $1^1\Pi_g$ ,  $1^1\Sigma_g^+$ , and  $1^1\Delta_g$ ) were involved in the associative ionization reaction [62]. The effects of all avoided crossings on the energy pooling process and on the associative ionization reaction between two excited potassium atoms  $\text{K}^*[4p]$  and between  $\text{Na}^*[3p]$  and  $\text{K}^*[4p]$  will be discussed in two forthcoming papers.

## ACKNOWLEDGMENTS

We want to thank M. Aubert-Frécon for a careful reading of this manuscript, and F. Masnou-Seeuws and O. Dulieu for stimulating discussions.

- [1] S. Magnier, Ph. Millié, O. Dulieu, and F. Masnou-Seeuws, *J. Chem. Phys.* **98**, 7113 (1993).
- [2] C. Amiot, *J. Mol. Spectrosc.* **146**, 370 (1991).
- [3] A. J. Ross, P. Crozet, J. D'Incan, and C. Effantin, *J. Phys. B* **19**, L145 (1986).
- [4] J. T. Kiu, C. C. Tsai, and W. C. Stwalley, *J. Mol. Spectrosc.* **171**, 200 (1995).
- [5] G. Jong, L. Li, T.-J. Whang, W. C. Stwalley, J. A. Coxon, M. Li, and A. M. Lyyra, *J. Mol. Spectrosc.* **155**, 115 (1992).
- [6] P. Kowalczyk, A. Katern, and F. Engelke, *Z. Phys. D* **17**, 47 (1990).
- [7] W. Jastrebski and P. Kowalczyk, *Chem. Phys. Lett.* **206**, 69 (1993).
- [8] L. Li, A. M. Lyyra, W. T. Luh, and W. C. Stwalley, *J. Chem. Phys.* **93**, 8452 (1990).
- [9] J. Heinze, U. Schühle, F. Engelke, and C. D. Caldwell, *J. Chem. Phys.* **87**, 45 (1987).
- [10] K. P. Huber and G. Herzberg, *Spectroscopic Constants of Diatomic Molecules* (Van Nostrand Reinhold, New York, 1979).
- [11] W. Jastrebski and P. Kowalczyk, *Chem. Phys. Lett.* **227**, 283 (1994).
- [12] A. J. Ross, C. Effantin, J. D'Incan, R. F. Barrow, and J. Vergès, *Ind. J. Phys.* **60B**, 309 (1986).
- [13] G. Jong and W. C. Stwalley, *J. Mol. Spectrosc.* **154**, 229 (1992).
- [14] G. Jong, H. Wang, C.-C. Tsai, W. C. Stwalley, and A. M. Lyyra, *J. Mol. Spectrosc.* **154**, 324 (1992).
- [15] A. J. Ross, C. Effantin, J. D'Incan, R. F. Barrow, and J. Vergès, *Ind. Mol. Phys.* **56**, 903 (1985); A. J. Ross, C. Effantin, J. D'Incan, and R. F. Barrow *Mol. Spectrosc.* **56**, 903 (1985).
- [16] A. J. Ross, R. M. Clements, and R. F. Barrow, *J. Mol. Spectrosc.* **127**, L546 (1988).
- [17] R. F. Barrow, R. M. Clements, G. Delacrétaz, C. Effantin, J. D'Incan, A. J. Ross, J. Vergès, and L. Wöste, *J. Phys. B* **20**, 3047 (1987).
- [18] J. Derouard and N. Sadeghi, *J. Chem. Phys.* **88**, 2891 (1988).
- [19] P. Kowalczyk, *J. Chem. Phys.* **91**, 2779 (1989).
- [20] H. Katô, M. Sakano, N. Yoshie, M. Baba, and K. Ishikawa, *J. Chem. Phys.* **93**, 2228 (1990).
- [21] M. Baba, S. Tanaka, and H. Katô, *J. Chem. Phys.* **89**, 7049 (1988).
- [22] S. Kasahara, M. Baba, and H. Katô, *J. Chem. Phys.* **94**, 7049 (1991).
- [23] A. J. Ross, Ph.D. thesis, Université Claude Bernard Lyon I, 1987 (unpublished).
- [24] A. J. Ross, C. Effantin, J. D'Incan, and R. F. Barrow, *J. Phys. B* **19**, 1449 (1986).
- [25] P. Kowalczyk, *J. Mol. Spectrosc.* **136**, 1 (1989).
- [26] S. Kasahara, H. Hikoma, and H. Katô, *J. Chem. Phys.* **100**, 63 (1994).
- [27] P. Kowalczyk, J. Derouard, and N. Sadeghi, *J. Mol. Spectrosc.* **151**, 303 (1992).
- [28] C. C. Tsai, T. J. Whang, J. T. Bahns, and W. C. Stwalley, *J. Chem. Phys.* **99**, 8480 (1993).
- [29] C. C. Tsai, J. T. Bahns, and W. C. Stwalley, *J. Chem. Phys.* **100**, 768 (1994).
- [30] T. Walker and P. Feng (unpublished).
- [31] A. Henriët and F. Masnou-Seeuws, *J. Phys. B* **21**, L339 (1988).
- [32] A. Henriët and F. Masnou-Seeuws, *J. Phys. B* **23**, 219 (1990).
- [33] G. H. Jeung, *J. Phys. B* **16**, 4289 (1983).
- [34] G. H. Jeung, *Phys. Rev. A* **35**, 26 (1987).
- [35] G. H. Jeung and A. J. Ross, *J. Phys. B* **21**, 1473 (1988).
- [36] G. H. Jeung, J. P. Daudey, and J. P. Malrieu, *Chem. Phys. Lett.* **94**, 300 (1983).
- [37] W. Müller and W. Meyer, *J. Chem. Phys.* **80**, 3311 (1984).
- [38] M. Foucrault, Ph. Millié, and J. P. Daudey, *J. Chem. Phys.* **96**, 1257 (1992).
- [39] C. Bottcher and A. Dalgarno, *Proc. R. Soc. London Ser. A* **340**, 187 (1974).
- [40] G. H. Jeung, J. P. Malrieu, and J. P. Daudey, *J. Chem. Phys.* **77**, 3571 (1982).
- [41] F. Spiegelmann, D. Pavolini, and J. P. Daudey, *J. Phys. B* **22**, 2465 (1989).
- [42] W. Müller, J. Flesch, and W. Meyer, *J. Chem. Phys.* **80**, 3297 (1984).
- [43] S. Magnier, M. Aubert-Frécon, O. Bouty, F. Masnou-Seeuws, Ph. Millié, and V. N. Ostrovskii, *J. Phys. B* **27**, 1723 (1994).
- [44] K. Krauss and W. J. Stevens, *J. Chem. Phys.* **93**, 4236 (1990).
- [45] W. J. Stevens, D. D. Konowalow, and L. B. Ratcliff, *J. Chem. Phys.* **80**, 1215 (1984).
- [46] E. Ilyabaev and U. Kaldor, *J. Chem. Phys.* **98**, 7126 (1993).
- [47] S. Gozzini, S. A. Abdullah, M. Allegrini, A. Cremoncini, and L. Moi, *Opt. Commun.* **63**, 97 (1987).
- [48] M. Allegrini, S. Gozzini, I. Longo, and P. Savino, *Nuovo Cimento* **1D**, 49 (1982).
- [49] Y. T. Lee and B. H. Mahan, *J. Chem. Phys.* **42**, 2893 (1965).
- [50] L. Brencher *et al.*, *Z. Phys. D* **10**, 211 (1988).
- [51] J. C. Barthelat and Ph. Durand, *Theor. Chim. Acta* **38**, 283 (1975).
- [52] D. Maynau and J. P. Daudey, *Chem. Phys. Lett.* **81**, 273 (1981).
- [53] C. E. Moore, in *Atomic Energy Levels*, edited by Editors, Natl. Bur. Stand. (U.S.) Circ. No. 467 (U.S. GPO, Washington, DC, 1949).
- [54] M. Broyer, J. Chevalyere, G. Delacrétaz, S. Martin, and L. Wöste, *Chem. Phys. Lett.* **99**, 206 (1983).
- [55] S. Leytweyler, A. Herrmann, L. Wöste, and E. Schumacher, *Chem. Phys.* **48**, 253 (1980).
- [56] D. L. Cooper, R. F. Barrow, J. Vergès, C. Effantin, and J. D'Incan, *Can. J. Phys.* **62**, 1543 (1984).
- [57] C. Linton, F. Martin, R. Bacis, and J. Vergès, *J. Mol. Spectrosc.* **137**, 235 (1989).
- [58] D. D. Konowalow and J. L. Fish, *Chem. Phys.* **77**, 435 (1983).
- [59] F. Engelke, *Faraday Discuss. Chem. Soc.* **71**, 357 (1981).
- [60] T. A. Patterson, H. Hotop, A. Kasdan, D. W. Norcross, and W. C. Lineberger, *Phys. Rev. Lett.* **32**, 189 (1974).
- [61] I. Yurova, O. Dulieu, S. Magnier, F. Masnou-Seeuws, and V. N. Ostrovskii, *J. Phys. B* **27**, 3659 (1994).
- [62] O. Dulieu, S. Magnier, and F. Masnou-Seeuws, *Z. Phys. D* **32**, 229 (1994).